

1 **Species dispersal mediates opposing influences of a branching network on**
2 **genetic variation in a metapopulation**

3

4 Ming-Chih Chiu¹, Bin Li¹, Kei Nukazawa², Thaddeus Carvajal¹ and Kozo Watanabe^{1,*}

5 ¹Department of Civil and Environmental Engineering, Ehime University, Ehime Prefecture

6 790-8577, Japan

7 ²Department of Civil and Environmental Engineering, University of Miyazaki, Miyazaki

8 Prefecture 889-2192, Japan

9

10 *Corresponding Author:

11 E-mail address: watanabe_kozo@cee.ehime-u.ac.jp

12

13 **Running Head:** Genetic effects of river branching

14 **Abstract**

15 In nature, ubiquitous fractal networks can have two but opposing influences, by increasing
16 distal and confluent habitats, respectively, under raising branching complexity on
17 metapopulations' genetic structure, although this remains poorly understood, particularly
18 regarding the roles of species-specific traits. In this study, we evaluated the integrated
19 influences of network complexity and species dispersal mode/ability on genetic divergence
20 among populations at the catchment scale, using a theoretical framework with empirical
21 genetic data from four sympatric stream macroinvertebrate species. Empirical patterns of
22 spatial genetic structure were attributed to dispersal ability and the species' habitat
23 specialisation levels. Our theoretical evidence showed that both greater landscape connectivity
24 (via shorter watercourse distance) and greater isolation of distal habitats (e.g. headwater
25 streams) occur in the more-branched networks. These two spatial features have negative and
26 positive influences on genetic divergence, respectively, with their relative importance varying in
27 different species. Watersheds harbouring a higher number of local populations have larger
28 genetic divergence of metapopulations. Downstream- and upstream-biased asymmetric
29 dispersals dictate increases and declines, respectively, in genetic divergence. In addition, distal
30 populations (e.g. in headwaters) have higher genetic independence between themselves under
31 higher levels of downstream-biased asymmetry. A strong association between species features
32 and evolutionary processes (gene flow and genetic drift) mediates the pervasive influences of

33 branching complexity on metapopulation genetic divergence, which highlights the importance
34 of considering species dispersal patterns when developing management strategies in rapid
35 environmental change scenarios.

36

37 **Keywords:** distribution, fractal geometry, habitat fragmentation, isolation by distance,
38 landscape complexity, macroinvertebrate

39

40 **Introduction**

41 There is growing interest in understanding how landscape architecture determines
42 ecosystems' spatial biodiversity (Economio & Keitt, 2008; Albert *et al.*, 2013; Wilson *et al.*,
43 2016). Despite comprehensive findings about spatial biodiversity, revealed by substantial
44 empirical and theoretical evidence (Chave, 2013), there is less information on spatial patterns
45 of intraspecific genetic diversity (Paz-Vinas *et al.*, 2015). Eco-evolutionary evidence and
46 theories derived from simplified landscapes are insufficient for understanding spatial genetic
47 patterns in complex systems such as rivers (Campbell Grant *et al.*, 2007; Thomaz *et al.*, 2016;
48 Terui *et al.*, 2018). Further explorations of the integrated genetic effects of species dispersal
49 and landscape connectivity on metapopulations (here defined as groups of subpopulations with
50 dispersal interactions) in complex habitats are needed.

51 In nature, ubiquitous fractal branching networks (e.g. with treelike patterns) have similar
52 structural features (Green, 2006), and species dispersal can mediate landscape genetic
53 structures (Paz-Vinas *et al.*, 2015; Thomaz *et al.*, 2016). Landscape connectivity shapes
54 evolutionary processes, such as gene flow and genetic drift, driving spatial patterns of
55 intraspecific genetic variation (McRae, 2006; Paz-Vinas *et al.*, 2015). Dendritic ecological
56 networks (e.g. riverscape structures) constrain species dispersal (Grant *et al.* 2007). For
57 example, ocean circulation patterns across seascapes shape their network connectivity and
58 intraspecific spatial genetic patterns (Braunisch *et al.*, 2010; Ruiz-Gonzalez *et al.*, 2015; Chust

59 *et al.*, 2016). The resulting spatial patterns within landscape networks are particularly
60 pronounced in species with low dispersal ability; for example, the genetic structures of sea
61 cucumbers (*Parastichopus californicus*) can be well explained by ocean circulation, which
62 mediates larvae dispersal (Xuereb *et al.*, 2018). Branching networks can be characterised by
63 distal and confluent habitats with fewer and more corridor linkages, respectively, and the two
64 types of habitat have positive and negative influences on genetic divergence among local
65 populations. Dendritic riverscape systems provide an excellent opportunity to reveal the roles
66 of species dispersal in opposing influences of branching fractals and resulting consequences
67 (i.e., either increasing or decreasing genetic divergence) based on their landscape spatial
68 configuration (described below in detail).

69 Dispersal asymmetry (the situation in which dispersal tendency between two habitats is
70 not necessarily equal to the tendency in the opposite direction) can dictate the isolation
71 processes between pairs of populations, which provides mechanisms behind widely
72 acknowledged patterns of spatial genetic diversity and differentiation (Kawecki & Holt, 2002).
73 In river and stream systems, species dispersal ability and distribution pattern mediate their
74 spatial genetic patterns (Pilger *et al.*, 2017). At all dispersal asymmetry levels,
75 streamflow-connected populations have habitat connectivity based on gene flows
76 predominantly in one direction or in both directions along a stream. Theoretically, more of
77 these isolated tributaries within a network, under high river conditions, result in higher genetic

78 differentiation between local populations (Thomaz *et al.*, 2016). For example, populations in a
79 river network's distal branches (e.g. different headwaters) are connected to a common source
80 population in downstream confluences. Therefore, downstream-biased dispersal (a tendency
81 for higher dispersal downstream than upstream) may lead to weak connections among
82 headwaters and a large genetic divergence among riverine species such as fish and
83 macroinvertebrates (Paz-Vinas *et al.*, 2013; Paz-Vinas & Blanchet, 2015).

84 In contrast, river branching can help enhance connectivity levels between demes by
85 naturally increasing the number of confluences and shortening their watercourse distances
86 (Labonne *et al.*, 2008). Stream-dwelling species with a strong tendency to migrate upstream,
87 such as aquatic insects that disperse by flying during their terrestrial adult stages (Petersen *et*
88 *al.*, 2004; Winterbourn *et al.*, 2007), can have low downstream-biased asymmetries or even
89 upstream-biased gene flow. In this case, there is weaker isolation between distal populations in
90 the river network when these sink populations receive higher gene flows from their shared
91 source population at downstream confluences.

92 In this study, we evaluated the combined influences of landscape network and species
93 dispersal on genetic divergences in ubiquitous fractal branching networks, which remain
94 poorly understood. To the best of our knowledge, this is the first study to address how dispersal
95 asymmetry mediates the countervailing influence of network branching with empirical genetic
96 data, by which genetic divergence can potentially increase or decrease within natural

97 populations depending on species dispersal. First, we explored the spatial genetic variation of
98 four macroinvertebrate species with flying adult stages in a shared river network, using a
99 mechanistic model, based on evolutionary processes and asymmetric dispersal in northeastern
100 Japan. These species all have substantially diverse habitat specificities and distributions within
101 the network (Watanabe *et al.*, 2014; Nukazawa *et al.*, 2015; Nukazawa *et al.*, 2017). Second,
102 with the model empirically validated through Bayesian inference, we theoretically evaluated
103 how branching complexity of random river networks, namely the network nodes' branching
104 prevalence (Terui *et al.*, 2018), differentially affects the global genetic differentiation
105 throughout catchments in the context of different asymmetric gene flow modes. Here, we
106 hypothesised that 1) widely distributed, generalist species associated with strong dispersal have
107 smaller genetic divergence than specialist species with clumped, patchy or disjunctive
108 distributions, and 2) increased river branching has positive effects on genetic divergence in
109 species with downstream-biased dispersal but the opposite (negative) effect in those with
110 symmetric dispersal, or upstream-biased asymmetric dispersal, which contributes to the
111 dispersal-mediated consequences of the opposite effects of network branching (isolated
112 habitats and landscape connectivity).

113

114 **Materials and methods**

115 *Empirical catchment and genetic data*

116 In the Natori and Nanakita Rivers in northeastern Japan (integrated catchment area c. 1200 km²;
117 Fig. 1), the flow regime exhibits a seasonal pattern, with flooding due to snowmelt in spring. In
118 the integrated catchment, the rivers flow from the western headwaters, at an elevation of 1350
119 m at Mount Kamuro, to the eastern river mouths at the Pacific Ocean, passing through Sendai
120 City with a population of one million. Approximately 60% of this area is forested and
121 mountainous. Two major reservoir dams (Kamafusa and Okura dams) are located there. The
122 regional lowlands are farmlands (13%, primarily with rice paddy fields) and a mixture of
123 residential and commercial areas (11%).

124 For both empirical and theoretical evidence, we used genetic data of neutral amplified
125 fragment length polymorphism (AFLP) markers from four macroinvertebrate species in this
126 catchment (Watanabe *et al.*, 2014). Three species were caddisflies (Trichoptera), namely,
127 *Hydropsyche orientalis*, *Stenopsyche marmorata* and *Hydropsyche albicephala*, while the
128 fourth was a mayfly, *Ephemera japonica* (Ephemeroptera). In this integrated catchment, the
129 species distributions vary considerably, from the widespread *H. orientalis* to the narrowly
130 distributed *E. japonica* (Fig. 1). These species have similar ecological functions in river
131 ecosystems by feeding on fine organic matter (< 1 mm diameter). Approximately 18 to 20
132 individuals collected at each sampling site were genotyped (128 to 473 polymorphic AFLP loci

133 for each species). Based on the locus-specific genetic differentiation across this catchment,
134 non-neutral loci identified by DFDIST (Beaumont & Nichols, 1996) and/or BayeScan (Foll &
135 Gaggiotti, 2008) were removed, and 98 to 449 neutral AFLP loci for each species (Fig. S1)
136 were retained and used for this study. Detailed protocols on the identification of non-neutral
137 loci are described in our previous report (Watanabe *et al.*, 2014).

138

139 *Metapopulation genetic modelling*

140 We developed a metapopulation genetic model based on isolation by distance (lower gene flow
141 with greater separation in terms of distance along the watercourse) and asymmetric dispersal
142 (upstream- and downstream-biased movements) between local populations. This model was
143 validated using the empirical data on neutral AFLP loci of the four macroinvertebrate species
144 in the catchment. With its parameters estimated by Bayesian inference, this model was used to
145 simulate the river branching influence on each species. We describe the model development
146 and Bayesian estimation of parameters below.

147 Given a single locus with two allelic types, labelled ‘1’ and ‘2’ (e.g. an AFLP), $z_{k,l}$
148 denotes the number of type ‘1’ alleles (number of individuals with the allele type) at locus l
149 from number of alleles $s_{k,l}$ (total number of types ‘1’ and ‘2’ together = total number of
150 individuals) observed in local population k . Here, neutral AFLP loci of individuals from local

151 populations were used as the observed modelling output. This random sampling process can be
152 characterised by a binomial distribution as follows (Guillot *et al.*, 2014):

153
$$z_{k,l} \sim \text{Binomial}(s_{k,l}, f_{k,l}) \quad [1]$$

154 where, in this local population, the frequency of allele ‘1’ is denoted by $f_{k,l}$. The allele
155 frequencies $z_{k,l}$ are independent between loci.

156 For each locus, the frequency of allele ‘1’ in local populations is determined by their
157 genetic variations (related to genetic drift), the watercourse distance between local populations
158 within the network (related to gene flow) and allele frequencies of the metapopulation. Without
159 genetic drift and natural selection, gene flow leads to the genetic homogeneity among local
160 populations, leading to allele frequencies at loci in local populations matching those of their
161 metapopulation (Andrews, 2010). We denote by $\theta_{k,l}$ the random deviation of
162 logit-transformed allele frequency in local populations from that of the metapopulation, and the
163 allele frequency $f_{k,l}$ is obtained from the inverse logit transformation as follows:

164
$$f_{k,l} = \text{invLogit}(\theta_{k,l} + m_{k,l}) = \frac{1}{1 + \exp(-(\theta_{k,l} + m_{k,l}))} \quad [2]$$

165 where m_{ij} denotes the metapopulation’s transformed allele frequency. The deviation $\theta_{k,l}$ can
166 be modelled by a multivariate normal distribution as follows (Bradburd *et al.*, 2013):

167
$$\theta_{k,l} \sim \text{MultiNormal}(\mu, \Omega) \quad [3]$$

168 where μ denotes the mean of zero, and the covariance matrix Ω is a function of the
169 watercourse distance between local populations and their spatial relationships (either

170 streamflow-connected or -disconnected). To model the covariance across local populations, we
171 modelled this as a function of the shortest watercourse distance along the river network h_{ij}
172 between populations i and j as follows (Ver Hoef & Peterson, 2010):

$$173 \quad \Omega_{ij} = \begin{cases} \underbrace{\sigma_D^2}_a + \underbrace{\sigma_U^2}_b + \sigma_G^2 & \text{if flow-connected and } i = j \\ \underbrace{\sigma_D^2 \exp(-c_D h_{ij})}_a + \underbrace{\sigma_U^2 \exp(-c_U h_{ij})}_b & \text{if flow-connected and } i \neq j \\ \underbrace{\sigma_U^2 \exp(-c_U h_{ij})}_b & \text{if flow-disconnected} \end{cases} \quad [4]$$

174 where part a or b describes the autocovariance, with the variance σ_D^2 or σ_U^2 and the scale
175 parameter c_D or c_U related to the downstream (D) or upstream (U) movement, respectively.
176 In part a , the autocovariance is set to zero for any two streamflow-disconnected populations
177 (e.g. local populations in different headwaters). In other words, streamflow-disconnected
178 populations are independent and have no gene flow between them via downstream movement.
179 The nugget variance σ_G^2 describes the random error.

180 In the Bayesian framework ‘Stan’ (Stan Development Team, 2014b), the R interface
181 ‘RStan’ (Stan Development Team, 2014a) was used to perform this metapopulation genetic
182 modelling. For each species, four Markov Chain Monte Carlo chains (for numerical
183 approximations of Bayesian inference) ran with 60,000 iterations each, and the first half of the
184 iterations for each chain were discarded as burn-in. This was determined by modelling
185 convergence when the R-hat statistic of each parameter approached a value of 1. To estimate
186 the model parameters, 2,000 samples obtained, by collecting one sample every 60 iterations for

187 each chain, were used to build the each parameter's posterior distribution.

188

189 *Simulation of river-branching influences*

190 Before the simulations, we created artificial river networks with varying branching

191 complexities (Terui *et al.*, 2018). The river networks were made up of nodes with scale length

192 e , with each node representing a local population. These nodes were assigned to be either

193 branching (or an upstream terminal) or non-branching with a probability of P or $1 - P$,

194 respectively. As a series of non-branching nodes terminated at a branching (or terminal) node.

195 The individual segments (watercourse stretches) were the geometric random variables with

196 branching probability P . Before merging the segments to create a river network, the drawing

197 process was repeated until the targeted number of notes (the number of local populations) and

198 an odd number of segments were reached. To create the river network, these segments were put

199 together as a pool merged hierarchically as follows (Fig. S2): Step 1) One segment was

200 randomly selected as the root and its upstream end was merged with the downstream end of

201 another two random segment selections. In this status, the semi-complete network had two

202 unmerged upstream ends each for the next possible merger. Step 2) Two more segments were

203 randomly selected and their downstream ends were merged together to the random draw one of

204 two (or even more at subsequent steps) unmerged upstream ends of the semi-complete network.

205 Step 3) Step 2 was repeated until there were no available segments in the pool.

206 We conducted stochastic simulations to illustrate the uncertainty of the global genetic
207 differentiation among local populations, G_{ST} (Nei, 1973), under river branching. We created
208 1,000 river networks (with scale length e equal to 1 km) with the branching probability P and
209 metapopulation size N (integer; the number of local populations in a river network) randomly
210 drawn from 0 to 1 and from 100 to 500, respectively. Our Bayesian model of each species with
211 median estimates was used to stimulate the global G_{ST} to be the metapopulation's genetic
212 divergence in each of the 1,000 random river networks. We performed this simulation using
213 the R packages 'stats' and 'base' (R Core Team, 2018).

214 Here, we built a regression model based on gradient boosting (GB) for each of the four
215 macroinvertebrate species, identifying the importance of 1) the fraction of any two local
216 populations being streamflow-disconnected in all combinations (any two being
217 streamflow-connected or -disconnected), 2) the mean watercourse distance between local
218 populations under different levels of river branching and 3) metapopulation size (number of
219 local populations) for genetic divergence (G_{ST}). GBs are a type of machine-learning algorithm
220 used for analysing unilinear relationships at the base of multiple decision trees and, in the
221 boosting process, each next tree model generated is added to improve on the performance of
222 the previous ensemble of models by minimising deviance (Friedman, 2001). Our GB
223 modelling was performed using the R package 'gbm' (Greenwell *et al.*, 2018), in which the
224 genetic divergence and other factors (the river features and metapopulation size) were

225 independent and dependent variables, respectively. We used the R package ‘dismo’ to assess
226 the optimal number of boosting trees via a cross-validation procedure (Hijmans *et al.*, 2017).
227 We illustrated how the downstream and upstream dispersal-related parameters of the
228 variances (σ_D^2 and σ_U^2 , respectively) or scales (c_D and c_U , respectively) influence river
229 branching on global genetic divergence. To illustrate this for each parameter type, we
230 considered 3×3 (nine) combinations of two parameters each with the same upper, median and
231 lower ends of ranges of their Bayesian median pooled estimates. For the same parameter type,
232 we replicated the nine combinations (see Fig. 5 and 6) in each of the 1,000 random river
233 networks, and parameters of the other type were fixed to the median of pooled estimates. In
234 addition to the variances and scales, each of the other model parameters was set to its Bayesian
235 median estimate.

236 **Results**

237 *Metapopulation genetic modelling*

238 Our Bayesian model was fitted to the empirical genetic data in the Natori and Nanakita
239 catchment, and the R^2 values derived from the residual (differences between the observed and
240 predicted numbers of type '1' alleles at a locus from the number of alleles observed in a local
241 population; see Formula 1) are 0.97, 0.98, 0.97 and 0.93 for *H. orientalis*, *S. marmorata*, *H.*
242 *albicephala* and *E. japonica*, respectively (Fig. 2). The metapopulation allele frequencies are
243 species-specific, and the variation of allele frequency is greater in the widespread *H. orientalis*
244 and *S. marmorata* than in the other two species with narrower habitat distributions (Fig. S1).
245 The pairwise genetic difference between empirical local populations tended to increase with
246 their watercourse distances throughout the four macroinvertebrate species (Fig. S3). Despite
247 substantial variation in the scale parameter, amplifying the isolating effect of distance across
248 study species (Fig. S4), there was a consistent decline in the genetic correlation between
249 populations (the covariance Ω_{ij} divided by the variance $\sigma_D^2 + \sigma_U^2 + \sigma_G^2$; see Formula 4) with
250 the increasing distance between local populations (Fig. S5). In addition, there was a greater
251 decline in the genetic correlation with distance in the widely distributed *H. orientalis* than in
252 the other species.

253

254 *River-branching influence*

255 We describe changes in the two landscape spatial configurations (fraction of any two local
256 populations being streamflow-disconnected in all combinations and mean watercourse distance
257 between local populations) with the increasing branching probability (P) in river networks (Fig.
258 3). Situations in which any two local populations are streamflow-disconnected (e.g. in different
259 tributaries) across metapopulations occur at higher rates in heavily branched river networks.
260 However, we found shorter watercourse distances between local populations in river networks
261 with higher branching probability. The metapopulation size (the number of interacting
262 subpopulations in a network) increases the values of both spatial configurations under the same
263 level of river branching.

264 Notably, changes in the values of the two spatial configurations act synergistically on the
265 genetic differentiation of metapopulations (G_{ST}) of the river network across four species (Fig.
266 4). Species-specific responses to the influence of river branching were identified. For example,
267 increased branching probability decreased the genetic divergence of the metapopulation for
268 three caddisflies (*H. orientalis*, *S. marmorata* and *H. albicephala*), but in the mayfly *E.*
269 *japonica*, the opposite response (higher genetic divergence) occurred. In addition, both a low
270 level and variation of genetic divergence are less likely to occur in the generalist *H. orientalis*
271 than in the other three species. The findings showed that the metapopulation size was
272 positively correlated to genetic divergence in all species. According to the GB modelling
273 results, the relative importance of streamflow-disconnected habitats, compared to the landscape

274 connectivity via a shorter watercourse distance, was higher in the mayfly *E. japonica* than in
275 the other three caddisfly species (Table 1).

276 The genetic performances, varying across species, were illustrated by how these model
277 parameters related to upstream and downstream dispersals take effect on the genetic
278 divergences (Fig. 5 and 6). Branching complexity has various impacts on genetic divergence,
279 which is determined by the relative values of the upstream and downstream parameters (scale
280 and variance in genetic covariation function, see Formula 4). The positive and negative
281 influences of branching complexity on the genetic divergence are conferred through the
282 relatively high and low values of the upstream-dispersal scale parameter compared to the
283 downstream one, respectively (Fig. 5). These, in turn, indicated higher and lower isolation
284 effects of watercourse distance between local populations, respectively. Lower genetic
285 divergence levels occurred in more-branched networks when there was higher variance related
286 to upstream movement (σ_U^2) than downstream movement (σ_D^2) (Fig. 6). In other words, the
287 populations in the distal branches (e.g. headwaters) have relatively strong genetic covariation
288 between themselves, particularly in complex river networks. In addition, river branching has
289 the opposite (positive) influence on the genetic divergences when σ_U^2 is lower than or equal to
290 σ_D^2 (Fig. 6).

291 **Discussion**

292 In this study, we explored the integrated role of landscape architecture and species
293 ecological strategy in shaping genetic divergence at neutral loci. We compared the landscape
294 genetics of sympatric macroinvertebrate species in river networks, based on our Bayesian
295 model, explicitly accounting for the effects of evolutionary processes among components of
296 metapopulations on the spatial genetic structure. This model indicated that river-network
297 connectivity predicted spatial genetic structures in four macroinvertebrate species. In addition,
298 their empirical structuring patterns were determined by the species' intrinsic factors
299 parameterised in this model. In this case, these factors can be associated with dispersal ability
300 and mode, species distribution and effective population size (associated with the genetic
301 variance in our model) in characterising relationships between genetic divergence and
302 landscape connectivity, as shown in the discussion below (see the subsequent section
303 '*Importance of species' intrinsic factors*').

304 In our simulations, these intrinsic factors could cause varying levels of overall genetic
305 differentiation in river networks and induced increased river branching to have different or
306 even opposite effects. Moreover, greater landscape connectivity (via shortened watercourse
307 distance) and higher distal habitat isolation (e.g. headwater streams) simultaneously occur in
308 more-branched river networks and have countervailing influences on genetic divergence; they
309 also have different levels of relative importance across these sympatric species. This can

310 provide extensive insights into other complex networks (e.g. highly fragmented landscapes or
311 those with corridors via ocean and atmospheric circulation). Our empirical and theoretical
312 results highlight the fundamental importance of considering species' biological traits, which
313 make different contributions to genetic connectivity, for the successful management of
314 ecological corridors.

315

316 *River branching and metapopulation genetic divergence*

317 In dendritic river networks, our simulation results showed a species-dependent change in
318 global genetic differentiation levels occurring with increases in network complexity and the
319 number of local populations in a metapopulation. We theoretically showed that the differential
320 downstream and upstream gene flows we considered in the model can act together to generate
321 such relationships. Our finding that increased populations in the river network enhanced
322 genetic differentiation is consistent with previous theoretical evidence (Thomaz *et al.*, 2016).
323 River branching's role has been documented, to some extent, in riverscape genetics, when
324 higher genetic diversity is observed in downstream populations than in upstream ones
325 (Paz-Vinas *et al.*, 2015) and greater river branching can increase the differences between such
326 populations (Thomaz *et al.*, 2016). Little or no gene flow imposed by high river branching,
327 because of strong isolation of headwater populations, can generally be observed for some
328 riverine species with high or intermediate levels of downstream-biased vagility, such as fish

329 species (Osborne *et al.*, 2014; Pilger *et al.*, 2017). By adopting our mechanistic model
330 validated by empirical data on macroinvertebrate species with flying adult stages, this
331 theoretical evidence reveals their dispersal ability to overcome riverscape constraints, leading
332 to low downstream-biased asymmetry and the opposite (negative) influence occurring under
333 increased river branching. In addition, our comprehensive consideration of various branching
334 river network topologies in simulations helped us to demonstrate the existence of opposing
335 influences co-occurring under branching complexity. In one early theoretical study, not
336 considering dispersal asymmetry (analogous to equal downstream and upstream dispersals in
337 our study), the dendritic network structure was also documented to promote low genetic
338 distances under high riverscape connectivity (Labonne *et al.*, 2008).

339

340 *Importance of species' intrinsic factors*

341 The river networks' architecture can be one important extrinsic factor for explaining the
342 observed and simulated genetic patterns, but there was strong variation among species with
343 different intrinsic factors in our study. This finding was also previously observed; for example,
344 two sympatric salmonid species were found to have remarkably different spawning locations,
345 mating systems and population sizes, and these biological traits mediated the influences of
346 riverscape features shaping their dispersal and genetic divergence in the Clark Fork River in
347 the USA (Whiteley *et al.*, 2004). For each upstream and downstream dispersal tendency in our

348 model, there are two parameters (scale and variance in the genetic covariation function; see
349 Formula 4) linked to species' intrinsic factors. In addition, these parameters together shape a
350 mechanism behind the countervailing influences of river branching on the genetic divergence
351 of metapopulations.

352 In our system, asymmetric (either downstream- or upstream-biased) dispersals could
353 determine the direction of the resulting influence on riverscape complexity. Stronger dispersal
354 can be associated with a lower value of the scale parameter since this parameter expands the
355 isolation effects of distance within river networks (see Formula 4). Our modelling results
356 showed that the widely distributed, generalist caddisfly (*H. orientalis*) has less intense genetic
357 divergence than other species with clumped, patchy or disjunctive distributions. In addition,
358 little change in genetic divergence, along with river branching, occurs in this caddisfly, which
359 can be explained by the low isolation effect by watercourse distance.

360 Furthermore, our results suggested that, in the mayfly species (*E. japonica*) with high
361 downstream-biased gene flow (based on a higher value of the scale parameter for upstream
362 than for downstream), as typically shown in fish species (e.g., Pilger *et al.*, 2017), river
363 branching has a positive influence on its genetic divergence, in which a higher number of
364 isolated distal branches in river networks (e.g. headwaters) occur under this dispersal
365 asymmetry. Mayfly species larvae are susceptible to drift during high river flow and have great
366 potential to be strong downstream dispersers (Nukazawa *et al.*, 2017). In our system, the

367 opposite (negative) influence of the branching network on the other three caddisfly species
368 with dispersal symmetry or even upstream-biased dispersal (based on the scale parameter for
369 upstream being similar to or higher than that for downstream, respectively; Fig. S4 and Fig. 5)
370 was identified. This might be attributable to their flying adults generally having a wide
371 dispersal range, showing strong terrestrial movement at least in the upstream direction. This
372 dampened the isolation between distal branches in river networks, compared to the case for
373 mayflies (or even stoneflies), exhibiting restricted distributions to areas very close to their
374 sources of emergence in the stream (Winterbourn *et al.*, 2007).

375 Besides dispersal abilities, the effective population size was revealed to be a factor
376 potentially influencing genetic drift and mediating the countervailing influences of river
377 branching in our study. In our model, the uncertainty regarding allele frequency, determined by
378 the variance parameter, can describe the levels of genetic drift, which can theoretically be
379 associated with the effective population size (Nei & Tajima, 1981). Observational studies have
380 documented that a smaller effective size of local populations can result in their higher genetic
381 differentiation, induced by genetic drift (Weckworth *et al.*, 2013; Richmond *et al.*, 2018). In
382 addition, there is an association between species features (dispersal ability and habitat
383 requirements) and genetic divergence (Phillipsen *et al.*, 2015). In our model, the variance
384 parameter can be separated into two parts related to upstream and downstream dispersals in the
385 genetic covariation function (Formula 4). Migration is one source of changes in population size,

386 and migrants themselves exhibit genetic variation derived from their source populations.
387 Different migrant population sizes can have varying influences on the genetic drift of sink
388 populations in the upstream or downstream direction. Therefore, the populations' locations (e.g.
389 in tributaries or the main stem) determine how immigration routes in upstream and/or
390 downstream directions act together in local populations, leading to their genetic drift. In our
391 mayfly species (*E. japonica*), for example, a higher value of downstream-related variance,
392 compared to the upstream one, theoretically determines the higher genetic variation among
393 local populations in distal branches of river networks (Fig. S4 and 6). As documented in both
394 theoretical and empirical studies, local populations of aquatic obligate species (e.g. fish
395 constrained to river channels) in main stem confluences experience less genetic drift than those
396 in isolated headwaters in river ecosystems (Thomaz *et al.*, 2016; Pilger *et al.*, 2017). As a result,
397 in cases with an increased number of tributaries and augmented river branching levels, there is
398 a higher likelihood that metapopulation genetic divergence will increase, for example, for this
399 mayfly species in our study or other downstream-biased species elsewhere (Osborne *et al.*,
400 2014).

401 From a conservation and management perspective that takes spatial genetic structure into
402 account (Luque *et al.*, 2012), it is crucial to understand the branching structure's role in driving
403 metapopulation genetic divergence. Dispersal can dictate differences in landscape genetic
404 diversification (Medina *et al.*, 2018), and predictive modelling, which can be validated by

405 empirical data based on asymmetric dispersals across networks, and shed light on the expected
406 impacts of global climate change and the consequences of management practices. To manage
407 native or even invasive species, our results shed light on the evolutionary importance of
408 dispersal abilities and modes, suggesting that these intrinsic factors should be considered in
409 decision-making processes when one managing strategy does not fit all species. For example,
410 the same management and conservation practices can produce different, or even the opposite,
411 results for species with varying levels of asymmetric gene flow and genetic drift (e.g. in
412 dendritic river systems).

413

414 **Acknowledgements**

415 This study was partly funded by the Japan Society for the Promotion of Science (JSPS). We

416 are grateful to Maribet Gamboa for her constructive comments on the manuscript.

417

418 **References**

- 419 Albert, E.M., Fortuna, M.A., Godoy, J.A., & Bascompte, J. (2013) Assessing the robustness of
420 networks of spatial genetic variation. *Ecol Lett*, **16 Suppl 1**, 86-93.
- 421 Andrews, C.A. (2010) Natural selection, genetic drift, and gene flow do not act in isolation in
422 natural populations. *Nature Education Knowledge*, **3**, 5.
- 423 Beaumont, M.A. & Nichols, R.A. (1996) Evaluating Loci for Use in the Genetic Analysis of
424 Population Structure. *Proceedings: Biological Sciences*, **263**, 1619-1626.
- 425 Bradburd, G.S., Ralph, P.L., & Coop, G.M. (2013) Disentangling the effects of geographic and
426 ecological isolation on genetic differentiation. **67**, 3258-3273.
- 427 Braunisch, V., Segelbacher, G., & Hirzel, A.H. (2010) Modelling functional landscape
428 connectivity from genetic population structure: a new spatially explicit approach.
429 *Molecular Ecology*, **19**, 3664-3678.
- 430 Campbell Grant, E.H., Lowe, W.H., & Fagan, W.F. (2007) Living in the branches: population
431 dynamics and ecological processes in dendritic networks. *Ecology Letters*, **10**, 165-175.
- 432 Chave, J. (2013) The problem of pattern and scale in ecology: what have we learned in
433 20 years? *Ecology Letters*, **16**, 4-16.
- 434 Chust, G., Villarino, E., Chenuil, A., Irigoien, X., Bizsel, N., Bode, A., Broms, C., Claus, S.,
435 Fernández de Puelles, M.L., Fonda-Umani, S., Hoarau, G., Mazzocchi, M.G., Mozetič,
436 P., Vandepitte, L., Veríssimo, H., Zervoudaki, S., & Borja, A. (2016) Dispersal similarly

- 437 shapes both population genetics and community patterns in the marine realm. *Scientific*
438 *Reports*, **6**, 28730.
- 439 Economo, E.P. & Keitt, T.H. (2008) Species diversity in neutral metacommunities: a network
440 approach. *Ecol Lett*, **11**, 52-62.
- 441 Foll, M. & Gaggiotti, O. (2008) A Genome-Scan Method to Identify Selected Loci Appropriate
442 for Both Dominant and Codominant Markers: A Bayesian Perspective. **180**, 977-993.
- 443 Friedman, J.H. (2001) Greedy function approximation: A gradient boosting
444 machine. *Ann. Statist.*, **29**, 1189-1232.
- 445 Green, D. (2006) *Complexity in Landscape Ecology*.
- 446 Greenwell, B., Boehmke, B., Cunningham, J., & Developers, G. (2018) *gbm: Generalized*
447 *Boosted Regression Models. R package version 2.1.4*.
- 448 Guillot, G., Vitalis, R., Rouzic, A.I., & Gautier, M. (2014) Detecting correlation between allele
449 frequencies and environmental variables as a signature of selection. A fast
450 computational approach for genome-wide studies. *Spatial Statistics*, **8**, 145-155.
- 451 Hijmans, R.J., Phillips, S., Leathwick, J., & Elith, J. (2017) *dismo: Species Distribution*
452 *Modeling. R package version 1.1-4*.
- 453 Kawecki, T.J. & Holt, R.D. (2002) Evolutionary consequences of asymmetric dispersal rates.
454 *The American Naturalist*, **160**, 333-347.
- 455 Labonne, J., Ravigné, V., Parisi, B., & Gaucherel, C. (2008) Linking dendritic network

- 456 structures to population demogenetics: The downside of connectivity. **117**, 1479-1490.
- 457 Luque, S., Saura, S., & Fortin, M.-J.J.L.E. (2012) Landscape connectivity analysis for
458 conservation: insights from combining new methods with ecological and genetic data.
459 **27**, 153-157.
- 460 McRae, B.H. (2006) Isolation by resistance. *Evolution*, **60**, 1551-1561.
- 461 Medina, I., Cooke, G.M., & Ord, T.J. (2018) Walk, swim or fly? Locomotor mode predicts
462 genetic differentiation in vertebrates. *Ecology Letters*, **21**, 638-645.
- 463 Nei, M. (1973) Analysis of gene diversity in subdivided populations. *Proceedings of the*
464 *National Academy of Sciences of the United States of America*, **70**, 3321-3323.
- 465 Nei, M. & Tajima, F. (1981) Genetic drift and estimation of effective population size. *Genetics*,
466 **98**, 625-40.
- 467 Nukazawa, K., Kazama, S., & Watanabe, K. (2015) A hydrothermal simulation approach to
468 modelling spatial patterns of adaptive genetic variation in four stream insects. *Journal*
469 *of Biogeography*, **42**, 103-113.
- 470 Nukazawa, K., Kazama, S., & Watanabe, K. (2017) Catchment-scale modeling of riverine
471 species diversity using hydrological simulation: application to tests of species-genetic
472 diversity correlation. *Ecohydrology*, **10**, e1778.
- 473 Osborne, M.J., Perkin, J.S., Gido, K.B., & Turner, T.F. (2014) Comparative riverscape genetics
474 reveals reservoirs of genetic diversity for conservation and restoration of Great Plains

- 475 fishes. **23**, 5663-5679.
- 476 Paz-Vinas, I. & Blanchet, S. (2015) Dendritic connectivity shapes spatial patterns of genetic
477 diversity: a simulation-based study. *Journal of Evolutionary Biology*, **28**, 986-994.
- 478 Paz-Vinas, I., Loot, G., Stevens, V.M., & Blanchet, S. (2015) Evolutionary processes driving
479 spatial patterns of intraspecific genetic diversity in river ecosystems. *Mol Ecol*, **24**,
480 4586-604.
- 481 Paz-Vinas, I., Quéméré, E., Chikhi, L., Loot, G., & Blanchet, S. (2013) The demographic
482 history of populations experiencing asymmetric gene flow: combining simulated and
483 empirical data. *Molecular Ecology*, **22**, 3279-3291.
- 484 Petersen, I., Masters, Z., Hildrew, A.G., & Ormerod, S.J. (2004) Dispersal of adult aquatic
485 insects in catchments of differing land use. **41**, 934-950.
- 486 Phillipsen, I.C., Kirk, E.H., Bogan, M.T., Mims, M.C., Olden, J.D., & Lytle, D.A. (2015)
487 Dispersal ability and habitat requirements determine landscape-level genetic patterns in
488 desert aquatic insects. *Molecular Ecology*, **24**, 54-69.
- 489 Pilger, T.J., Gido, K.B., Propst, D.L., Whitney, J.E., & Turner, T.F. (2017) River network
490 architecture, genetic effective size and distributional patterns predict differences in
491 genetic structure across species in a dryland stream fish community. *Mol Ecol*, **26**,
492 2687-2697.
- 493 R Core Team (2018) *R: A Language and Environment for Statistical Computing*. R Foundation

- 494 for Statistical Computing, Vienna, Austria. <https://www.R-project.org/>.
- 495 Richmond, J.Q., Backlin, A.R., Galst-Cavalcante, C., O'Brien, J.W., & Fisher, R.N. (2018)
- 496 Loss of dendritic connectivity in southern California's urban riverscape facilitates
- 497 decline of an endemic freshwater fish. **27**, 369-386.
- 498 Ruiz-Gonzalez, A., Cushman, S.A., Madeira, M.J., Randi, E., & Gómez-Moliner, B.J. (2015)
- 499 Isolation by distance, resistance and/or clusters? Lessons learned from a forest-dwelling
- 500 carnivore inhabiting a heterogeneous landscape. **24**, 5110-5129.
- 501 Stan Development Team (2014a) *RStan: the R interface to Stan, Version 2.5*.
- 502 <http://mc-stan.org/rstan.html>.
- 503 Stan Development Team (2014b) *Stan Modeling Language Users Guide and Reference Manual,*
- 504 *Version 2.5.0*.
- 505 Terui, A., Ishiyama, N., Urabe, H., Ono, S., Finlay, J.C., & Nakamura, F. (2018)
- 506 Metapopulation stability in branching river networks. *Proc Natl Acad Sci U S A*, **115**,
- 507 E5963-E5969.
- 508 Thomaz, A.T., Christie, M.R., & Knowles, L.L. (2016) The architecture of river networks can
- 509 drive the evolutionary dynamics of aquatic populations. *Evolution*, **70**, 731-739.
- 510 Ver Hoef, J.M. & Peterson, E.E. (2010) A moving average approach for spatial statistical
- 511 models of stream networks. *Journal of the American Statistical Association*, **105**, 6-18.
- 512 Watanabe, K., Kazama, S., Omura, T., & Monaghan, M.T. (2014) Adaptive genetic divergence

- 513 along narrow environmental gradients in four stream insects. *PLoS One*, **9**, e93055.
- 514 Weckworth, B.V., Musiani, M., Decesare, N.J., McDevitt, A.D., Hebblewhite, M., & Mariani,
515 S. (2013) Preferred habitat and effective population size drive landscape genetic
516 patterns in an endangered species. *Proc Biol Sci*, **280**, 20131756.
- 517 Whiteley, A.R., Spruell, P., & Allendorf, F.W. (2004) Ecological and life history characteristics
518 predict population genetic divergence of two salmonids in the same landscape. **13**,
519 3675-3688.
- 520 Wilson, M.C., Chen, X.-Y., Corlett, R.T., Didham, R.K., Ding, P., Holt, R.D., Holyoak, M., Hu,
521 G., Hughes, A.C., Jiang, L., Laurance, W.F., Liu, J., Pimm, S.L., Robinson, S.K., Russo,
522 S.E., Si, X., Wilcove, D.S., Wu, J., & Yu, M. (2016) Habitat fragmentation and
523 biodiversity conservation: key findings and future challenges. *Landscape Ecology*, **31**,
524 219-227.
- 525 Winterbourn, M.J., Chadderton, W.L., Entekin, S.A., Tank, J.L., & Harding, J.S. (2007)
526 Distribution and dispersal of adult stream insects in a heterogeneous montane
527 environment. *Fundamental and Applied Limnology / Archiv für Hydrobiologie*, **168**,
528 127-135.
- 529 Xuereb, A., Benestan, L., Normandeau, É., Daigle, R.M., Curtis, J.M.R., Bernatchez, L., &
530 Fortin, M.-J. (2018) Asymmetric oceanographic processes mediate connectivity and
531 population genetic structure, as revealed by RADseq, in a highly dispersive marine

532 invertebrate (*Parastichopus californicus*). *Molecular Ecology*, **27**, 2347-2364.

533

534

535 **Table 1.** Performance measures and relative importance of predictors in gradient boosting models for *Ephemera japonica* (EJ), *Stenopsyche marmorata*,
 536 *Hydropsyche orientalis* (HO) and *Hydropsyche albicephala* (HA), in which the simulated genetic divergence of the metapopulation (global G_{ST}) is the
 537 response variable and fraction of any two local populations streamflow-disconnected, mean watercourse distance between populations and
 538 metapopulation size are predictor variables.

Species	Number of trees	Model performance		Relative importance (%)		
		RMSE	R ²	Streamflow-disconnected fraction	Watercourse distance	Metapopulation size
EJ	2250	0.03	0.94	90.4	4.5	5.1
HA	800	0.06	0.88	1.0	95.1	3.9
HO	600	0.05	0.64	4.3	85.3	10.4
SM	650	0.03	0.65	6.0	79.4	14.6

539 **Figure legends**

540 **Fig. 1.** The study catchment and distribution of (a) *Ephemera japonica* (EJ), (b) *Hydropsyche*
541 *albicephala* (HA), (c) *Hydropsyche orientalis* (HO) and (d) *Stenopsyche marmorata* (SM) in
542 northeastern Japan.

543 **Fig. 2.** Observed and predicted numbers of type '1' alleles at a locus from the number of alleles
544 observed in a local population (see Formula 1) for (a) *Ephemera japonica* (EJ), (b)
545 *Hydropsyche albicephala* (HA), (c) *Hydropsyche orientalis* (HO) and (d) *Stenopsyche*
546 *marmorata* (SM) with posterior distribution in Bayesian modelling.

547 **Fig. 3.** Theoretical predictions for relationships of (a) mean watercourse distance between
548 populations or (b) fraction of any two streamflow-disconnected populations (e.g. in headwaters)
549 in all combinations with branching complexity under differential metapopulation sizes (range:
550 100 to 500, number of local populations).

551 **Fig. 4.** Theoretical predictions for relationships between metapopulation genetic divergence
552 (global G_{ST}) and branching complexity under differential metapopulation sizes (range: 100 to
553 500, number of local populations) for (a) *Ephemera japonica* (EJ), (b) *Hydropsyche*
554 *albicephala* (HA), (c) *Hydropsyche orientalis* (HO) and (d) *Stenopsyche marmorata* (SM).

555 **Fig. 5.** Theoretical predictions for relationships between metapopulation genetic divergence
556 (global G_{ST}) and branching complexity under differential metapopulation sizes (range: 100 to
557 500, number of local populations) for combinations of dispersal-related scale parameters in

558 genetic covariation function (Formula 4), including (a, e and i) $c_D = c_U$, (b, c and f) $c_D < c_U$,

559 and (d, g and h) $c_D > c_U$.

560 **Fig. 6.** Theoretical predictions for relationships between metapopulation genetic divergence

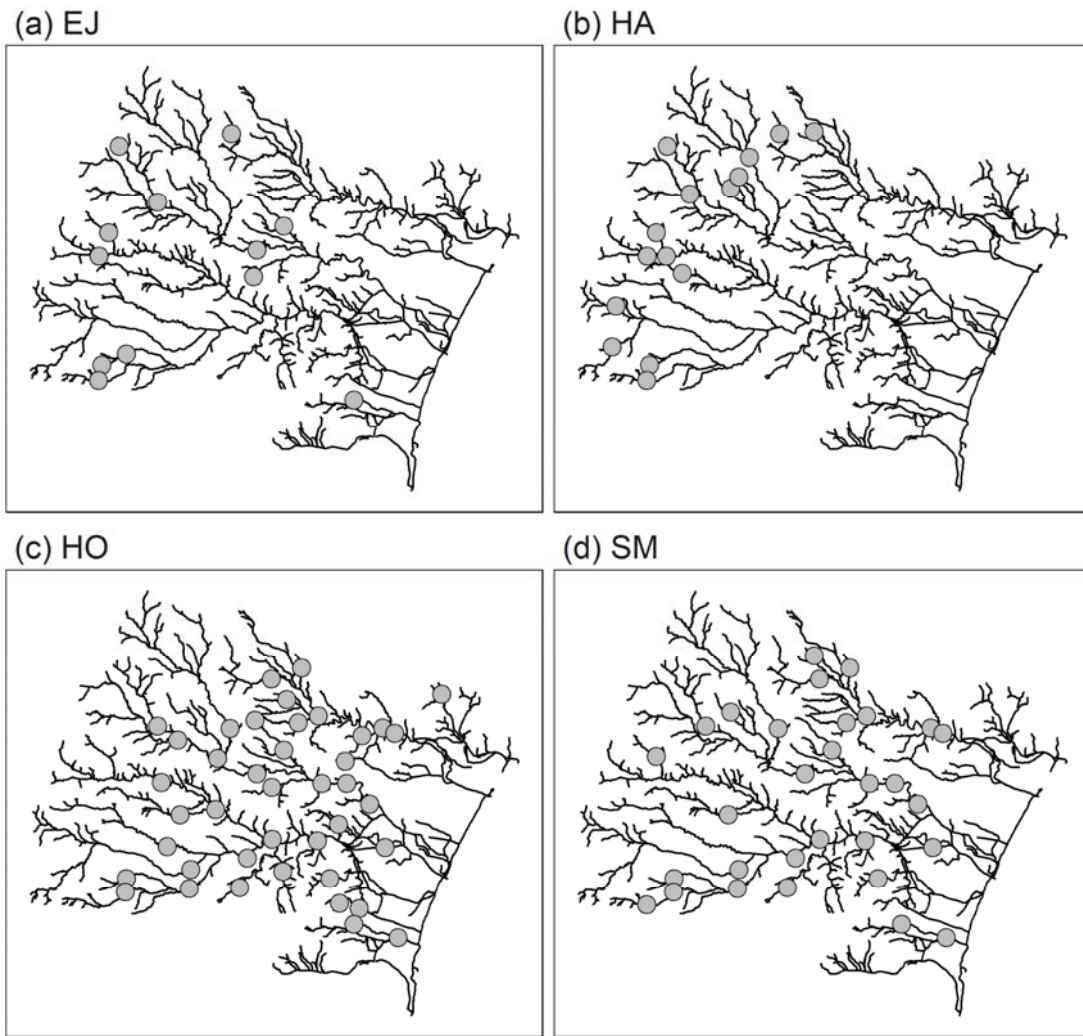
561 (global G_{ST}) and branching complexity under differential metapopulation sizes (range: 100 to

562 500, number of local populations) for combinations of dispersal-related variances in genetic

563 covariation function (Formula 4), including (a, e and i) $\sigma_D^2 = \sigma_U^2$, (b, c, and f) $\sigma_D^2 < \sigma_U^2$ and (d,

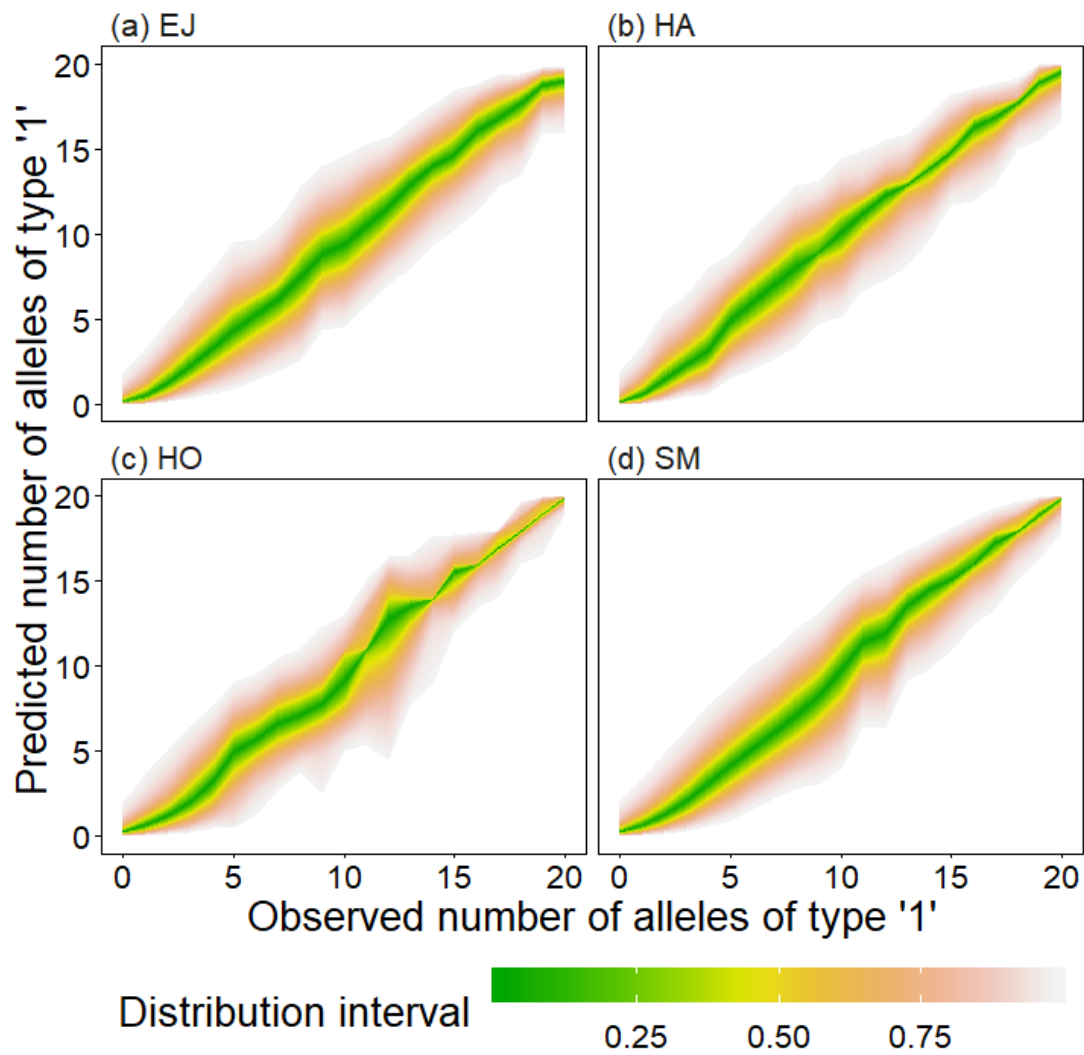
564 g and h) $\sigma_D^2 > \sigma_U^2$.

565



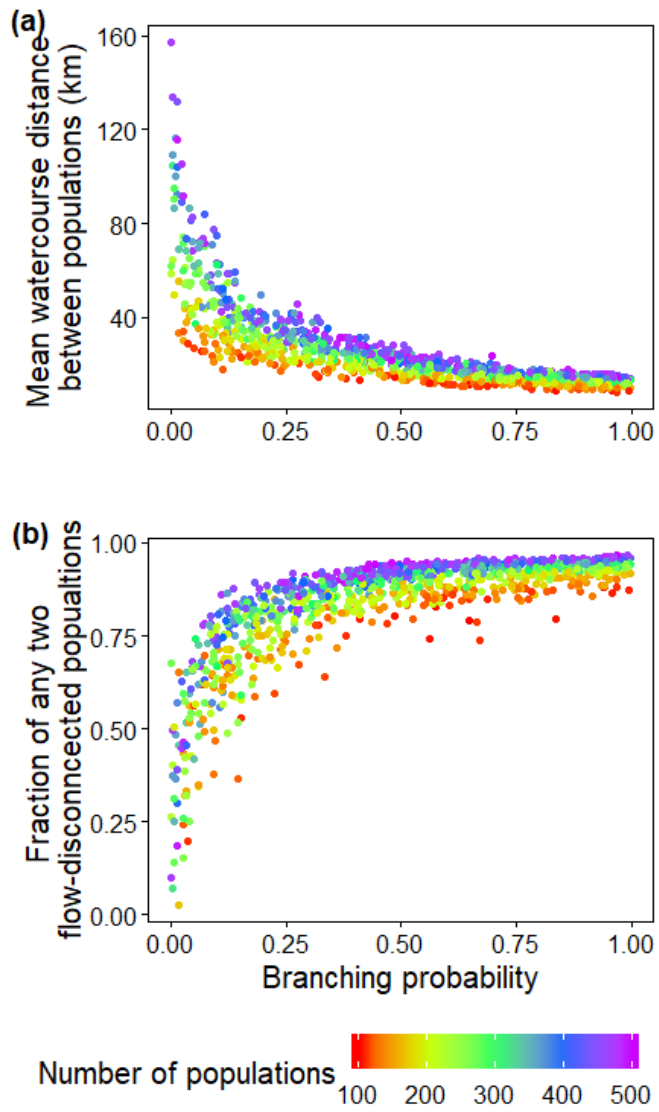
566

567 **Fig. 1**



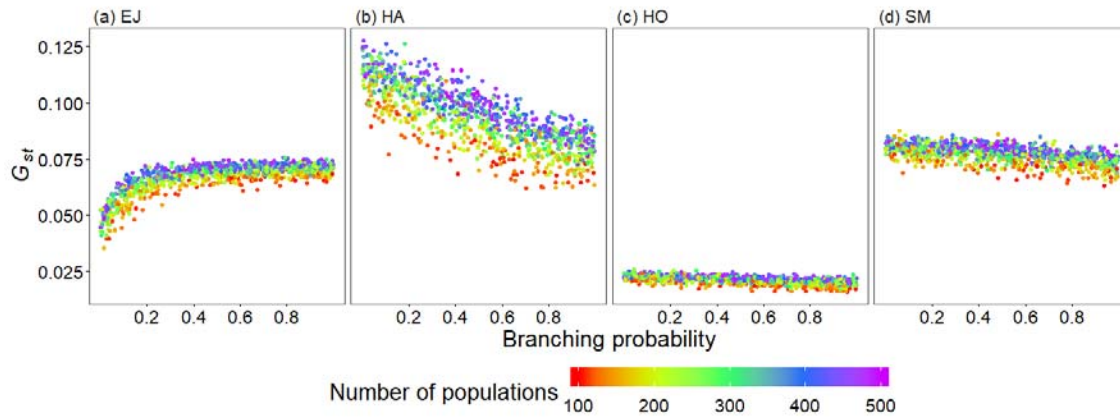
568

569 **Fig. 2**



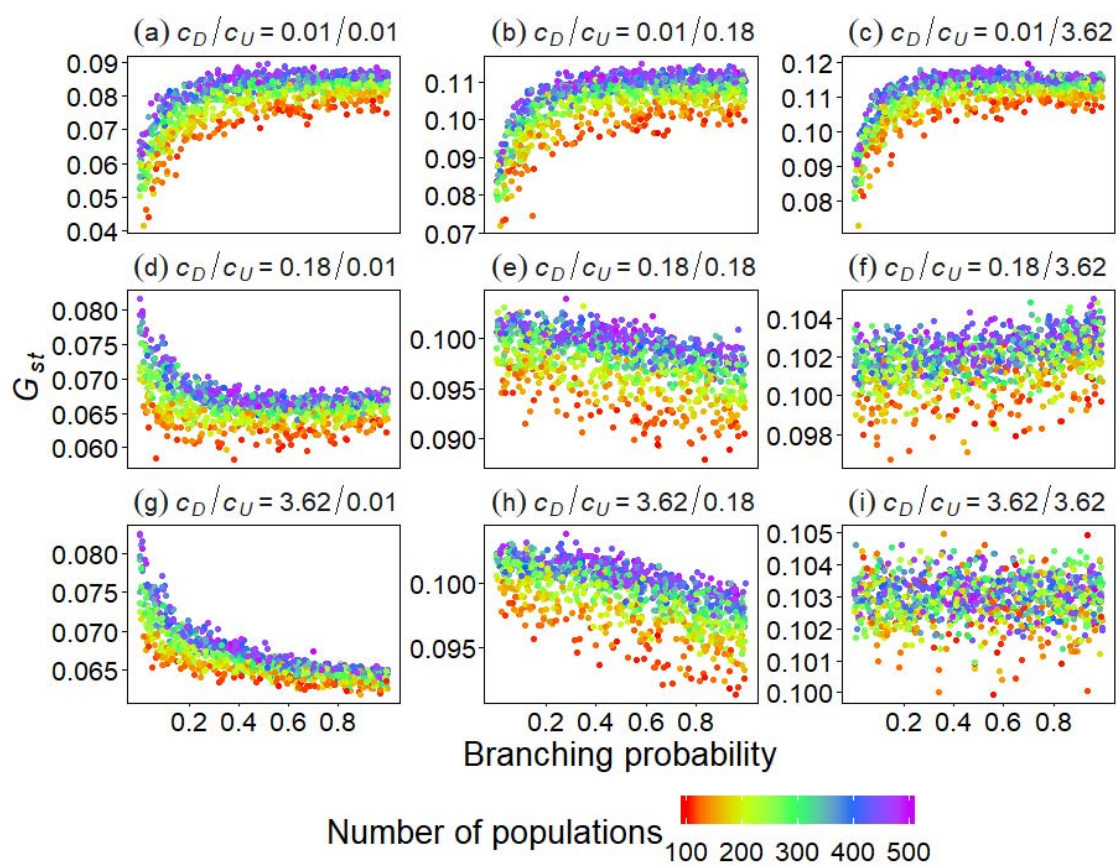
570

571 **Fig. 3**



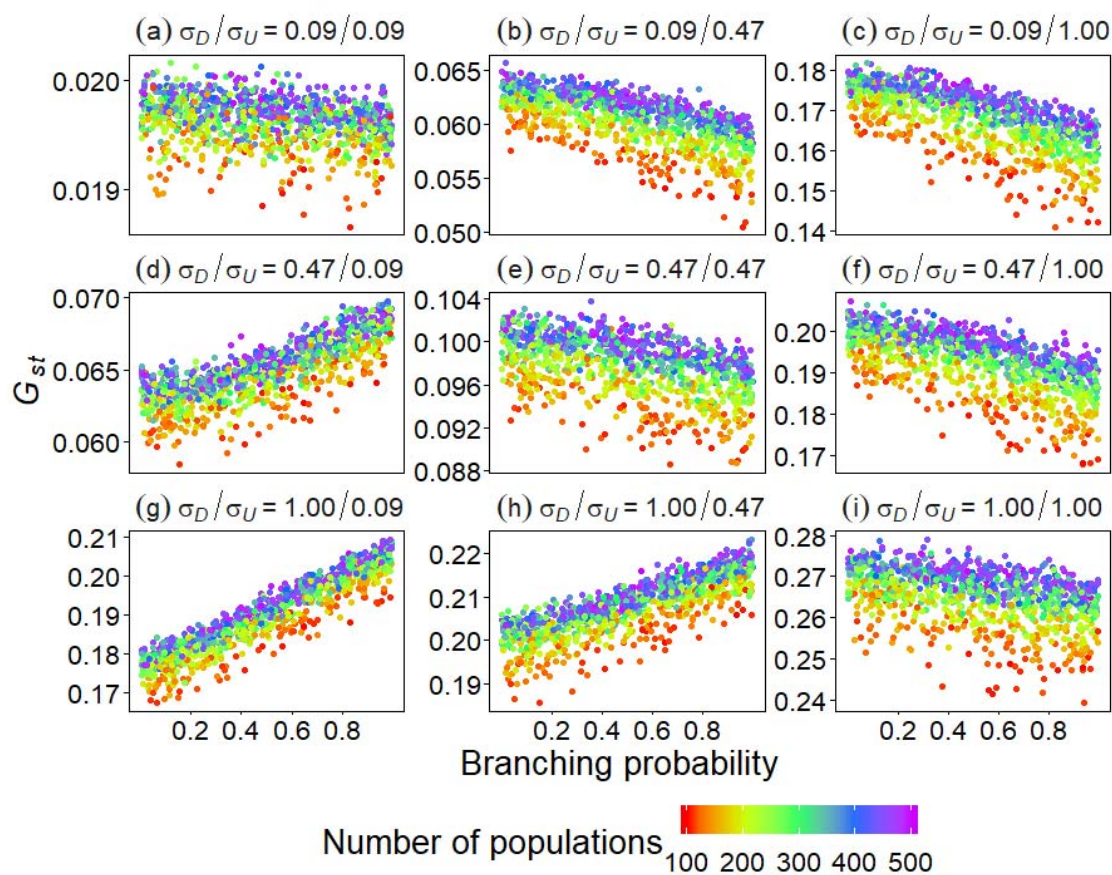
572

573 **Fig. 4**



574

575 **Fig. 5**



576

577 **Fig. 6**